Received: 29 December 2021 | Revised: 21 March 2022 | Accepted: 26 March 2022

DOI: 10.1111/gcb.16188

Global Change Biology WILEY

TECHNICAL ADVANCE

Positron-emitting radiotracers spatially resolve unexpected biogeochemical relationships linked with methane oxidation in Arctic soils

Michael P. Schmidt[1,2] | Steven D. Mamet[1] | Curtis Senger[1] | Alixandra Schebel[1] | Mitsuaki Ota[1] | Tony W. Tian[1] | Umair Aziz[3] | Lisa Y. Stein[4] | Tom Regier[5] | Kevin Stanley[3] | Derek Peak[1] | Steven D. Siciliano[1]

[1]Department of Soil Science, University of Saskatchewan, Saskatoon, Saskatchewan, Canada

[2]USDA-ARS United States Salinity Laboratory, Riverside, California, USA

[3]Department of Computer Science, University of Saskatchewan, Saskatoon, Saskatchewan, Canada

[4]Department of Biological Sciences, University of Alberta, Edmonton, Alberta, Canada

[5]Canadian Light Source, Inc., Saskatoon, Saskatchewan, Canada

Correspondence
Michael P. Schmidt, USDA-ARS United States Salinity Laboratory, 450 W Big Springs Road, Riverside, CA 92507, USA.
Email: mike.schmidt@usda.gov

Funding information
Federated Cooperatives Limited, Grant/Award Number: 537285-18; Sylvia Fedoruk Canadian Centre for Nuclear Innovation, Grant/Award Number: J2018-0041; Canada Foundation for Innovation; Natural Sciences and Engineering Research Council of Canada; University of Saskatchewan; Government of Saskatchewan; Western Economic Diversification Canada; National Research Council Canada; Canadian Institutes of Health Research

Abstract

Arctic soils are marked by cryoturbic features, which impact soil-atmosphere methane (CH_4) dynamics vital to global climate regulation. Cryoturbic diapirism alters C/N chemistry within frost boils by introducing soluble organic carbon and nutrients, potentially influencing microbial CH_4 oxidation. CH_4 oxidation in soils, however, requires a spatio-temporal convergence of ecological factors to occur. Spatial delineation of microbial activity with respect to these key microbial and biogeochemical factors at relevant scales is experimentally challenging in inherently complex and heterogeneous natural soil matrices. This work aims to overcome this barrier by spatially linking microbial CH_4 oxidation with C/N chemistry and metagenomic characteristics. This is achieved by using positron-emitting radiotracers to visualize millimeter-scale active CH_4 uptake areas in Arctic soils with and without diapirism. X-ray absorption spectroscopic speciation of active and inactive areas shows CH_4 uptake spatially associates with greater proportions of inorganic N in diapiric frost boils. Metagenomic analyses reveal *Ralstonia pickettii* associates with CH_4 uptake across soils along with pertinent CH_4 and inorganic N metabolism associated genes. This study highlights the critical relationship between CH_4 and N cycles in Arctic soils, with potential implications for better understanding future climate. Furthermore, our experimental framework presents a novel, widely applicable strategy for unraveling ecological relationships underlying greenhouse gas dynamics under global change.

KEYWORDS
Arctic soils, carbon cycling, greenhouse gases, methane fluxes, methane oxidation, methanotrophy, nitrogen cycling, radioisotopes, soil biogeochemistry

1 | INTRODUCTION

Extensive permafrost thawing is currently underway in Arctic soils due to disproportionate Arctic region warming (Biskaborn et al., 2019). Previously frozen soil organic carbon (SOC) pools are entering active biogeochemical cycles and may be converted to greenhouse gases (GHGs; e.g., CO_2, CH_4; Biskaborn et al., 2019; Schuur & Abbott, 2011; Schuur et al., 2015). Up to 195 Pg C in the form of GHGs could be released from permafrost soils by 2100, with 2.03–6.21 Pg C from CH_4 emissions (Schuur et al., 2013). CH_4 represents approximately 30% of the total radiative forcing

Michael P. Schmidt and Steven D. Mamet contributed equally to this work.

from permafrost C emissions over the same period, highlighting the critical role of CH_4 dynamics in Arctic soils (Schuur et al., 2013). Moist SOC-rich Arctic cryosols under anaerobic conditions and abundance of low molecular weight organic acids promote methanogenesis, which favors net soil CH_4 emission and relatively high soil CH_4 concentrations (Yang et al., 2016). CH_4 emissions may be mitigated by methanotrophic bacteria, which assimilate and oxidize CH_4 as a C source. In the case of SOC-rich cryosols, low-affinity methanotrophs requiring CH_4 concentrations higher than atmospheric concentrations (>100s ppmv compared with ≈1.8–2 ppmv, respectively) may mitigate CH_4 emissions, however these soils generally serve as net CH_4 sources (Baani & Liesack, 2008; Oh et al., 2020). In contrast, mineral-rich cryosols such as those found in Artic deserts (≈26% of Arctic land area) are lower in SOC, moisture and CH_4 emissions than organic-rich cryosols (Whalen & Reeburgh, 1990). In mineral cryosols, high-affinity methanotrophs can actively take up CH_4 at atmospheric CH_4 concentrations (Rusley et al., 2019; Tveit et al., 2019). Accordingly, mineral cryosols serve as an important CH_4 sink and play a key role in regulating Arctic CH_4 dynamics as a net CH_4 sink (Emmerton et al., 2014; Juncher Jørgensen et al., 2015; Lau et al., 2015; Oh et al., 2020). A 47% increase in CH_4 uptake by polar desert soils is projected by 2100, suggesting mineral soils represent a critical offset to predicted rising GHG emissions from organic rich Arctic soils (Curry, 2009).

In Arctic soils, microbial CH_4 oxidation is highly variable depending on local conditions of soil moisture, redox potential, and nutrient speciation (e.g., Cu, N, P; Gray et al., 2014; Knapp et al., 2007; Perryman et al., 2020; Zhang et al., 2019). Furthermore, evidence suggests dissolved organic carbon (DOC) species in soils may play an important role in regulating CH_4 oxidation in dry ecosystems (Sullivan et al., 2013). Within the context of Arctic desert soils, all these factors are influenced by widespread cryoturbic features, which locally alter soil moisture and nutrient, SOC, and DOC speciation. This results from freeze-thaw processes, which can lead to concentric size-sorted features known as frost boils (i.e., frost heaving) as well as upward injection of DOC and nutrients from subsoils into higher soil horizons (i.e., diapirism), which may influence GHG dynamics (Brummell et al., 2015; Ota et al., 2020; Walker et al., 2004). For example, reduction in CH_4 fluxes by cryoturbic diapirism have been linked to lower substrate availability and reduced SOC degradability (Ota, 2021).

Defining methanotrophic relationships and biogeochemical environments within soil media is complicated by the spatially heterogeneous distribution of soil properties and, therefore, biological activity at various spatial scales (Baveye et al., 2018). Non-destructive, positron-emitting radiotracers can spatially resolve biological activity in soils (Kinsella et al., 2012; Thorpe et al., 2019; Vandehey et al., 2014). Positron-emitting radionuclides undergo a radioactive decay known as positron emission through which a parent nuclide proton converts to a neutron, yielding a positron (${}^{0}_{1}\beta$) and daughter atom (Equation 1). Positrons next undergo annihilation with electrons in the surrounding medium, producing two gamma rays (Equation 2; L'Annunziata, 2012).

$$ {}^{X}_{Z}A \rightarrow {}^{0}_{1}\beta + {}^{X}_{z-1}B, \tag{1} $$

$$ {}^{0}_{1}\beta + {}^{0}_{-1}\beta \rightarrow \gamma + \gamma. \tag{2} $$

Positrons or emitted gamma radiation may be detected to spatially delineate radiotracer distribution. Use of positron-emitting radiotracers for spatially resolving microbiological activity in soils presents many advantages over activity-based assays or other imaging strategies. The short half-life of positron-emitting radiotracers (minutes to hours for several commonly applied radionuclides) limits tracer incorporation to active processes. Radiotracer-based imaging applies exceptionally low concentrations of chemically equivalent tracers, minimizing disturbance to system chemistry while allowing for non-destructive spatial resolution of activity within intact natural media (Schmidt et al., 2020). Here, we use positron-emitting $[^{11}C]CH_4$ as a functional tracer to pinpoint micron to millimeter-scale soil CH_4 uptake through radiographic imaging of emitted ${}^{0}_{1}\beta$. Active soil sample regions are then extracted for metagenomic and spectroscopic C/N speciation analyses to investigate the link between active microbial CH_4 oxidation and local biogeochemical factors in diapiric and non-diapiric Arctic desert soils. Given observed relationships between GHG emissions and local SOC speciation in Arctic and Subarctic soils, we hypothesize that diapirism will induce spatial association between microbial CH_4 oxidation and distinct SOC species in these Arctic desert soils. Our novel radiotracer-guided spectroscopic and metagenomic analysis framework is used to probe this hypothesis of diapirism-induced spatial association between microbial CH_4 oxidation and SOC speciation in Arctic desert soils. We aim to better understand ecological factors that moderate biological CH_4 uptake in Arctic soils with respect to soil spatial heterogeneity. However, the range of radiotracers available as well as flexibility of dosing and downstream analyses are compatible with several processes relevant to global change ecology in a range of environmental systems (Schmidt et al., 2020).

2 | MATERIALS AND METHODS

2.1 | Field site and soil sampling description

Soils were collected from a High Arctic desert plateau 5 km southwest of Alexandra Fjord (78°51′N, 75°54′W) on Ellesmere Island, Nunavut (Bliss et al., 1994; Ota et al., 2020). Annual precipitation averages <50 mm and mean annual temperature ranges from −16 to −19°C (Bliss et al., 1994; Ota et al., 2020). Soils are classified as Regosolic Turbic Cryosols, reflecting weak horizon development, low SOC content, and cryoturbic frost boils across the field site (Brummell et al., 2012). Soils were sampled from diapiric and non-diapiric frost boils. Diapiric frost boils

were delineated by an SOC increase greater than 0.2 log(%) in subsurface soils as determined by field visible and near-infrared reflectance spectrometry, indicating subsurface organic matter intrusion (Guy et al., 2015; Muller et al., 2017). Non-diapiric frost boils were classified by the absence of a subsurface SOC increase. Soils were collected from two diapiric and two non-diapiric frost boils developed on dolomite and granite. In diapiric frost boils, soils were collected from depths corresponding to the highest SOC content within diapiric features and comparable depths from non-diapiric frost boils. An additional soil used for probing the uptake of $[^{11}C]CH_4$ by a sterilized soil matrix was collected from a non-diapiric frost boil on dolomitic parent material. The dominant soils at the Alexandra Fiord Dome site are Regosolic Turbic Cryosol or Turbic Cryosols have very high (25%–39% by mass) contents of coarse fragments (>2 mm), which preclude maintaining soil structure during collection and transport from field-to-lab (Canadian Agricultural Services Coordinating Committee, National Research Council Canada, & Canada, 1998; Food & Agriculture Organization of the United Nations, 2014; Muller et al., 2022). After collection, soil samples were frozen and stored at −20°C until use. Once in the laboratory, coarse fragments (pebbles and rocks) were removed for reproducible radiographic imaging. Before use in this study, soils were air dried at room temperature for 48 h and then sieved to <2 mm. In so doing, we disrupted gross soil structure but retained aggregate soil structures that are the focus of this study. Basic soil properties may be found in Table S1.

2.2 | $[^{11}C]CH_4$ synthesis

$[^{11}C]CO_2$ ($^{11}Ct_{1/2}$ = 20.3 min) was produced by the $^{14}N(p, \alpha)^{11}C$ reaction through bombardment of a 99.5% N_2, 0.5% O_2 gas target with 18MeV protons for 5 min with a TR-24 cyclotron (Advanced Cyclotron Systems, Inc.) located at the Saskatchewan Centre for Cyclotron Sciences. This process yields a gas mixture, including radioactive ^{11}C and ^{13}N species, which required purification for $[^{11}C]CO_2$ isolation and $[^{11}C]CH_4$ production. Nitrogen oxides were first trapped and removed using a previously described method (Tewson et al., 1989). $[^{11}C]CO_2$ was then collected on a 4 Å molecular sieve mixed with silica-supported nickel catalyst for separation from residual $[^{13}N]N_2$. To produce $[^{11}C]CH_4$ from captured $[^{11}C]CO_2$, the molecular sieve/catalyst trap with adsorbed $[^{11}C]CO_2$ was pressurized to 135 kPa with 99.9% H_2 and heated to 350°C. After 2 min, synthesized $[^{11}C]CH_4$ was released using an air push gas. Unreacted $[^{11}C]CO_2$ was removed from this gas stream by an Ascarite trap (Thomas Scientific) and subsequently directed to a dosing chamber or gas bag for further application. $[^{11}C]CH_4$ yields were generally on the order of 1×10^{-11} moles for our synthesis and purification system. Soils were, therefore, assumed to be dosed with CH_4 at concentrations approximating atmospheric CH_4 concentration, as the concentration of added $[^{11}C]CH_4$ is several orders of magnitude lower than atmospheric CH_4.

2.3 | Validating microbial $[^{11}C]CH_4$ uptake

Validation studies of $[^{11}C]CH_4$ uptake by methanotrophic bacteria used the model methanotrophic bacterium *Methylomonas methanica* (American Type Culture Collection (ATCC), 51626) grown in 160 ml serum bottles containing 70 ml of nitrate mineral salts medium (ATCC medium 1306). Bottles initially had a 50% air and 50% CH_4 headspace. Cultures were grown to mid exponential growth stage before $[^{11}C]CH_4$ uptake studies. Triplicate (n = 3) bottles containing active *M. methanica* cultures, autoclaved *M. methanica* exponential growth phase cultures, and autoclaved growth medium without *M. methanica* inoculation were used to evaluate $[^{11}C]CH_4$ uptake through biotic and abiotic processes. Active *M. methanica* and controls were dosed with $[^{11}C]CH_4$ by removing 22.7 ml of headspace gas from bottles and immediately adding 22.7 ml of $[^{11}C]CH_4$ in air drawn from a gas bag containing $[^{11}C]CH_4$, resulting in an approximately 63% air and 37% CH_4 headspace. Bottles were then incubated for 1.5 h at room temperature. After incubation, 11.3 ml of culture or uninoculated growth medium was withdrawn from bottles and placed in a well counter for radioactivity determination.

2.4 | Soil incubation, dosing with $[^{11}C]CH_4$ and imaging

Prior to $[^{11}C]CH_4$ dosing, soils were incubated to activate microbiota. 14.5 g of dried and sieved soils were placed in polyethylene holders (50 mm diameter × 5.7 mm depth) and hydrated to 40% water filled pore space. Soils were then incubated at 25°C for 3 days, with water content maintained by daily additions of water as needed. A set of soils was sterilized after initial incubation using propylene oxide fumigation to test the influence of abiotic processes on uptake of $[^{11}C]CH_4$ by soils (Wolf & Skipper, 2018). After incubation, soils were placed in a sealed chamber for $[^{11}C]CH_4$ dosing. Once soils were in the sealed chamber, air containing trace amounts of $[^{11}C]CH_4$ was flowed into the chamber and dosed for 30 min.

Radiographic imaging of $[^{11}C]CH_4$ uptake by soils entails an exposure and revelation step to produce a two-dimensional image of radiotracer distribution. Soil samples were placed against an autoradiographic imaging film (Storage Phosphor Screen BAS-IP MS E2025, Cytiva Life Sciences) in the dark and exposed for 30 min. Films were then stored in a cassette until image revelation (within 24 h) to prevent light exposure. Image revelation from exposed films was performed by scanning films (Typhoon imaging system; Cytiva Life Sciences) and subsequently digitizing images.

2.5 | Image processing and extraction of active and background soils

Autoradiographic images were processed using the Fiji distribution of ImageJ (Abràmoff et al., 2004; Schindelin et al., 2012).

[^{11}C]CH_4 image pairs were cropped and co-registered with non-soil background pixels removed. Pixel values were rescaled based on the radioactivity present at the time of imaging to facilitate activity comparisons among soils. For example, pixel values for one image initially ranged from 15 to 20,858 (unsigned 16-bit data, so the max is 2^{16} or 65,536). The activity of synthesized [^{11}C]CH_4 was 2.88 GBq/L, so pixel values were rescaled from 0 to 28,800. Images were imported into ERDAS Imagine (V9.23, Leica Geosystems) where unsupervised machine learning clustered similar pixels and to codify low-, medium-, and high-radioactivity regions in each soil (unsupervised classification, Iterative Self-Organizing Data Analysis algorithm, 15 iterations, 0.99 convergence, 30 classes, post-hoc merge to three classes; Irvin et al., 1997; Tou & Gonzalez, 1974).

After classifying soil CH_4 uptake activity regions, soil aliquots were extracted from samples for x-ray absorption near-edge structure (XANES) and metagenomic analyses. Aluminum spacers (4.5 mm OD, 3.2 mm ID, and 4 mm deep; McMaster-Carr, Prod. No. 94669A097) were pressed with alcohol-sterilized tweezers into areas corresponding to one low (background) and two high (active) activity regions per sample for extraction. Prior to downstream analyses, extracted soils within spacers were pressed with an alcohol-sterilized stainless-steel piston for stability.

2.6 | X-ray absorption spectroscopic analysis

Pressed soil samples were mounted without further modification for XANES analysis on the 11ID-1 Spherical Grating Monochromator beamline at the Canadian Light Source (Saskatoon, Saskatchewan, Canada). All post-hoc modifications to C and N spectra were performed in Athena (Ravel & Newville, 2005). C and N K-edge XANES spectra were deconvoluted and relative C/N functional group concentrations were determined using a Gaussian curve fitting procedure in Fityk (Fityk V1.2.1; Dhillon et al., 2017; Wojdyr, 2010). C spectra were fit with components corresponding with unsaturated/quinone, aromatic, phenolic/heterocyclic/substituted aromatic/ketone, aliphatic, carboxylic, alkyl/alcohol/ether, and carbonate C functionalities (Table S2; Dhillon et al., 2017; Gillespie et al., 2015; Myneni, 2002). N spectra were fit with components corresponding with N in 6 and 5 member heterocyclic aromatic, amide, pyrazole/pyrrole/urea, five member rings with unpaired electrons, aromatic substituent groups, inorganic, and alkyl bonding environments (Table S2; Gillespie et al., 2011; Leinweber et al., 2007; Myneni, 2002; Urquhart et al., 1995). Further details regarding collection, processing, and analysis of XANES spectra are found in the Supporting Information. Low sample numbers probed for each treatment combination, due to limitations of synchrotron-based spectroscopic approaches, prevented rigorous statistical analyses of XANES data. Further considerations regarding statistics and spatial relationships in X-ray absorption analysis, see Dynes et al., 2015.

2.7 | Soil DNA extraction and sequencing

DNA was extracted from isolated regions of active [^{11}C]CH_4 uptake for downstream metagenomic analyses. For comparison against inactive soils, DNA was extracted from bulk soils, rather than isolated background regions, to ensure enough DNA was obtained. Soil DNA was isolated from soil samples using the FastDNA™ SPIN Kit (MP Biomedicals). Extracted DNA was quantified using a Qubit® 2.0 fluorimeter with dsDNA HS Assay Kit (ThermoFisher).

DNA quality and average fragment length were determined using TapeStation with Genomic DNA reagents (Agilent). Libraries were constructed using an Illumina DNA prep kit with 16 unique dual indices (Illumina) and quantified by a Qubit dsDNA BR assay kit (Invitrogen). Library pools were diluted for optimal cluster density against a 1%PhiX control. A High Output kit was used with a NextSeq 550 sequencer system (Illumina) to generate approximately 350 million yield pairs for downstream quality filtering and analyses.

2.8 | Shotgun metagenomic sequencing analyses

SqueezeMeta v. 1.2.0 pipelines were used for assembly, taxonomic, functional, and bin analyses (Tamames & Puente-Sánchez, 2019). The pipelines used the co-assembly mode option to pool reads before assembly using Megahit (Li et al., 2015). Functions were assigned using Diamond Blastx alignments of reads against Clusters of Orthologous Groups of proteins and KEGG databases using lowest common ancestor and fun3 methods (Buchfink et al., 2015; Clark et al., 2016; Huson et al., 2007; Kanehisa, 2000; Tatusov et al., 2003).

To remedy some of the pitfalls associated with genomic data, we applied a series of data filters (Figures S1 and S2) to ensure a robust dataset with sufficient inferential power (Allen et al., 2016; Hua et al., 2019; Mamet et al., 2021; Qin et al., 2020; Schimel & Schaeffer, 2012). Following data filtering, taxa abundance data were converted to relative abundances. Initial analyses indicated little difference between microbial composition and diversity of [^{11}C]CH_4 hotspots (Figure S3), so these data were combined and compared with microbial communities in bulk soils. Taxonomic relationships were probed using a cladogram produced using the ape package in R (package v. 5.4-1) and visualized using ggtree v. 2.2.4 (Paradis & Schliep, 2019; Yu, 2020).

The number of taxa estimated using contigs was 4428 and reduced to 183 through data filtering (Figure S1). Taxa classified to genus but not to species were merged for each genus (e.g., "Unclassified *Burkholderia*" and "*Burkholderia* sp.") and similar for taxa classified to Phylum but no further (e.g., genus: "Unclassified Actinobacteria," and species: "Actinobacteria bacterium" or "Unclassified Actinobacteria"). This agglomeration further reduced the number of taxa to 76. Here we specifically found a *Ralstonia* species (*R. pickettii*) was 149-fold more abundant in hotspots (M = 12%) relative to background (0.08%) and was highly connected to other taxa (Figure S4). Therefore, we explored KEGG pathways related to

C, CH_4, and N metabolism in *Ralstonia* bins. Of the 81 pathways of interest, 18 were present in *Ralstonia*. We then compared normalized abundance of KEGG genes related to C, CH_4 and N in *Ralstonia* bins using generalized linear models. Additional details related to metagenome data classification, filtering, and gene abundance comparisons are found in the Supporting Information. It should be noted that in this study, we elected to use non-amplicon-based methods to avoid primer biases with the drawback that rare but important members of the community may be screened out.

3 | RESULTS

3.1 | [^{11}C]CH_4 is a suitable radiotracer to visualize biotic soil CH_4 uptake

Radioactivity measurements of active cultures and controls showed a greater uptake of [^{11}C]CH_4 by active *M. methanica* cultures relative to sterile growth media and autoclaved *M. methanica* cultures (Figure 1) after incubating 1.5 h. This suggests isotopic substitution of ^{12}C with ^{11}C did not preclude biological CH_4 oxidation and that the radioactivity levels applied were low enough to not halt biological activity. Abiotic [^{11}C]CH_4 uptake into control solutions occurred to a lower extent than in active *M. methanica* cultures. Although CH_4 does not partition strongly into aqueous solutions ($k_H^\circ = 1.3 \times 10^{-3}$ mol kg^{-1} bar^{-1}), the high CH_4 concentration in headspaces likely favored some CH_4 solvation (Linstrom, 1997).

These findings extended to the validation of radiographic imaging methodology used in our study. Radiographic images of an active and a sterilized control soil collected from our field site showed that the active soil uniformly took up [^{11}C]CH_4, whereas the same soil matrix subject to fumigant sterilization did not appear to retain [^{11}C]CH_4 (Figure 1). This indicates that abiotic CH_4 uptake by soils is negligible compared with biotic uptake under conditions employed here and imaged [^{11}C]CH_4 uptake regions likely represent zones of biological CH_4 uptake.

3.2 | CH_4 uptake in Arctic desert soils is heterogeneous at sub-millimeter to millimeter scales

Radiographic imaging of [^{11}C]CH_4 uptake by diapiric and non-diapiric soils revealed active CH_4 uptake in all soils (Figure 2). Activity was spatially heterogenous and localized within distinct regions ranging from the submillimeter to millimeter scale. Diapirism does not seemingly influence the size or distribution of biologically active CH_4 uptake sites. Given the uniform hydration of soils, and the soil dosing methods, spatial heterogeneity of CH_4 uptake is likely driven by localized microbiological and/or biogeochemical, rather than physical, factors in our system. At the atmospheric CH_4 concentrations implemented for dosing all soils, it is likely that imaged uptake regions correspond with high-affinity methanotrophic activity rather than low-affinity methanotrophy. Low-affinity methanotrophs would unlikely be able to efficiently assimilate CH_4 under dosed concentrations.

Prior to localized XANES biogeochemical speciation and metagenomic analysis of soils, raw radiographic images were classified on a continuum of [^{11}C]CH_4 uptake (Figure 2). To compare C/N biogeochemistry and microbiology between biologically active and background regions of soils, aliquots corresponding with background (low) and active (high) [^{11}C]CH_4 uptake were extracted from each imaged soil for XANES and metagenomic analyses (Figure 3).

3.3 | Positron-emitting radiotracers spatially link CH_4 oxidation with distinct N speciation

SOC speciation was not influenced by diapirism or CH_4 uptake activity. Similar to a previous study on Subarctic SOC characterization,

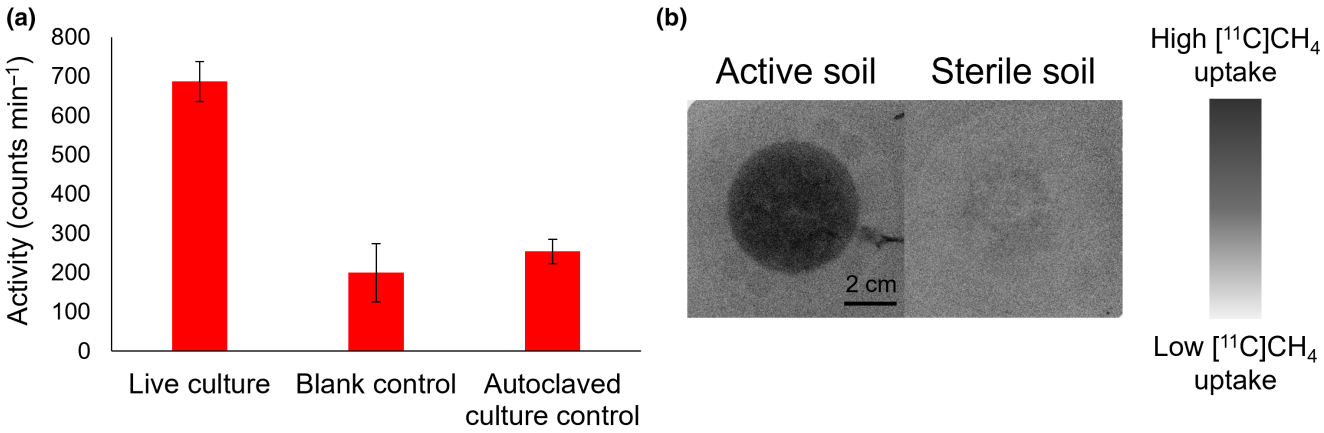

FIGURE 1 (a) Radioactivity measurements of live inoculated, uninoculated, and autoclaved control inoculated growth media after 1.5 h incubation with a 63% air/37% CH_4 headspace labelled with trace [^{11}C]CH_4 ($n = 3$). Error bars represent standard deviations from the mean. (b) Radiographic images of an active and fumigated Arctic desert soil incubated with air labelled with trace [^{11}C]CH_4 for 30 min

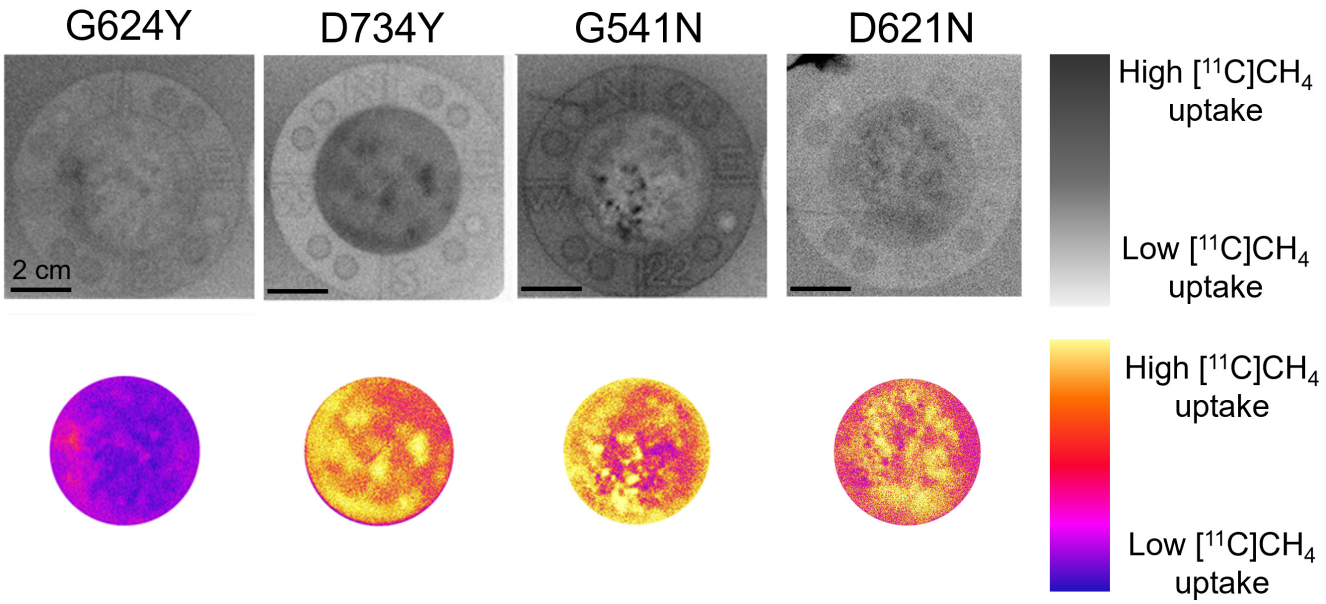

FIGURE 2 Raw (top) and classified (bottom) radiographic images of $[^{11}C]CH_4$ uptake by Arctic desert soils. Dolomitic and granitic parent material are denoted in sample codes by D and G, respectively. The presence of diapiric (Y) or absence of diapiric features (N) in soils is also denoted by sample codes

speciation shows prevalence of carboxyl, aliphatic, aromatic, and heterocyclic/phenolic/ketone organic SOC (i.e., excluding carbonate features) functional groups in these Arctic soils (Figure S5a–d; Dhillon et al., 2017; Gillespie et al., 2014; Myneni, 2002). Spectrum areas corresponding with functional groups generally follow a trend of carboxyl > aliphatic ≈ aromatic ≈ heterocyclic/phenolic/ketone > alkyl C-O > quinone/unsaturated C (Figure S5a–d). Averaged across all extracted background and active uptake soil aliquots from diapiric and non-diapiric soils, all functional groups correspond with similar spectral proportions, suggesting SOC speciation is not influenced by diapirism (Figure S5a).

Diapirism influenced N speciation in these soils. N speciation in non-diapiric soils was dominated by inorganic N species (e.g., NH_4^+ and NO_3^-) with smaller contributions from organic N functional groups (e.g., heterocyclic N, N bound to aromatic species and amide N; Figure S6a; Gillespie et al., 2011; Leinweber et al., 2007; Myneni, 2002; Urquhart et al., 1995). Diapiric soils had a lower inorganic N proportion relative to non-diapiric frost boils, with a higher proportion of organic N functionalities in diapiric soils, specifically N bound to aromatic groups, N with unpaired electrons in ring structures, and N within five-member heterocycles. N speciation differences between background and active $[^{11}C]CH_4$ uptake regions across imaged soils were modest compared with the effect of diapirism on N speciation (Figure S6b). More constrained comparison between N species on diapiric and non-diapiric frost boils indicates diapirism influences spatial association between active and background soil regions (Figure 4). Diapirism favors a spatial association between methanotrophy and greater proportion of inorganic N.

3.4 | Positron-emitting radiotracers spatially resolve taxonomic and functional traits related to CH_4 metabolism in active soils

The SqueezeMeta pipeline produced 640,518,010 reads in total, ranging from 22,517,278 to 100,905,292 reads per sample (sample mean = 53,376,501). Rarefaction curves indicated sufficient coverage depth, levelling at approximately 2,000,000 reads (Figure S7). Data filtering reduced the number of KEGG pathways and taxa by 69% and 96%, respectively (Figure S1). Interestingly, proteobacterial taxa previously associated with high-affinity methanotrophy in soils were absent in the filtered dataset (Holmes et al., 1999; Lau et al., 2015; Tveit et al., 2019). This suggests other taxa may play an active role in CH_4 uptake in these soils. Of the filtered species, *R. pickettii* was present in relatively high abundances in soil regions corresponding to $[^{11}C]CH_4$ uptake across all soils 149-fold relative to bulk soils (12% vs. 0.08%; Figure 5). Several other taxa were notably differentially abundant between the two soils (>100-fold), though were of sufficiently low relative abundances (<0.5%) that downstream analyses focused on *R. pickettii*.

Several CH_4 metabolism-related genes detected within *R. pickettii* were enriched in $[^{11}C]CH_4$ uptake hotspots relative to bulk soils. Gene enrichment related to direct CH_4 uptake (e.g., particulate methane monooxygenase) may have occurred in non-diapiric samples with *pmoC* only detected at ≈1 tpm in $[^{11}C]CH_4$ uptake regions. Trace detection in four distinct $[^{11}C]CH_4$ uptake regions compared with absence in background indicates biologically meaningful detection. In diapiric soils, *pmoC* (present at ≈75 tpm) did not differ between background and $[^{11}C]CH_4$ uptake hotspots.

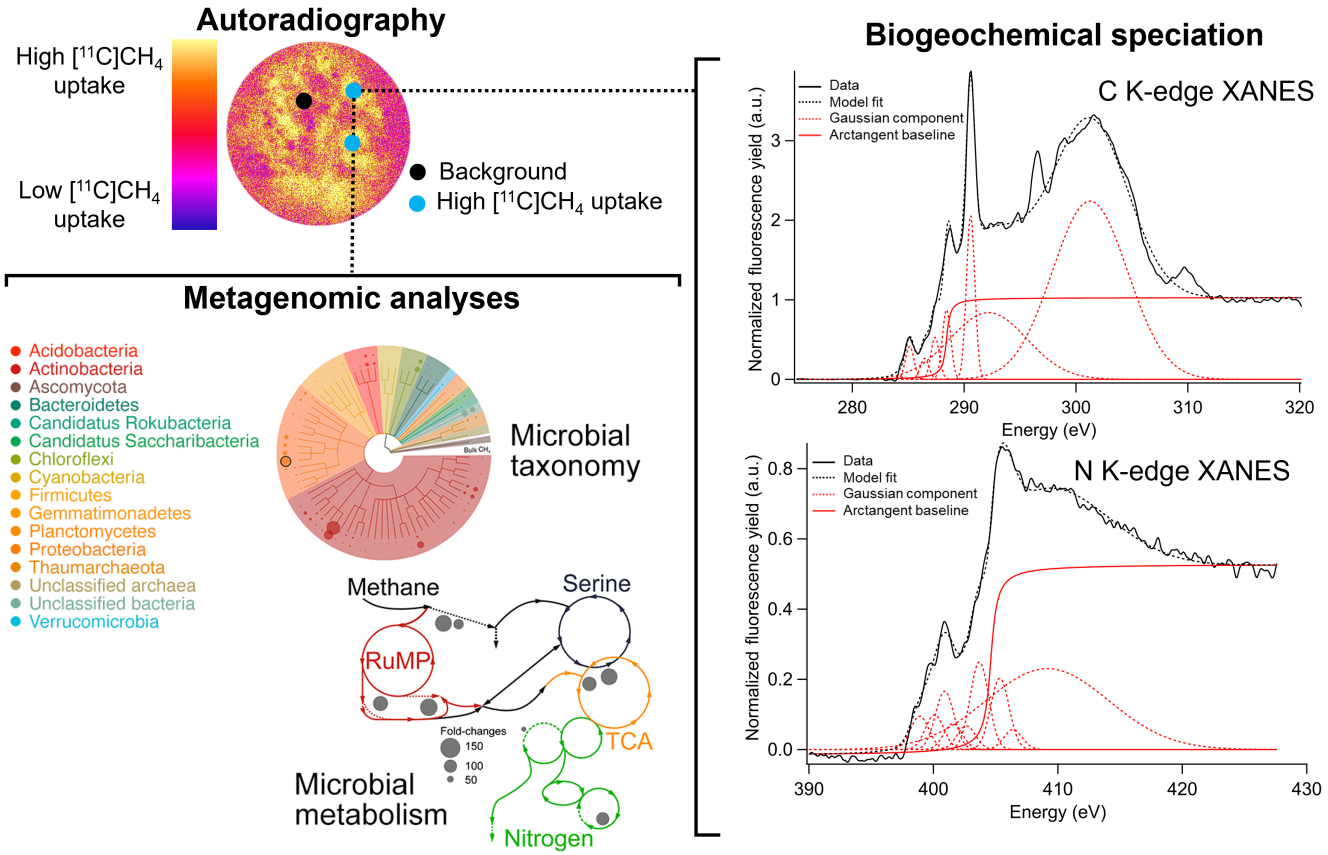

FIGURE 3 Experimental framework diagram showing processed radiographic image with delineated background and active [$^{11}CH_4$] uptake soil regions, representative C- and N-XANES spectra with model components from an active soil aliquot and outputs from metagenomic analyses from extracted soils

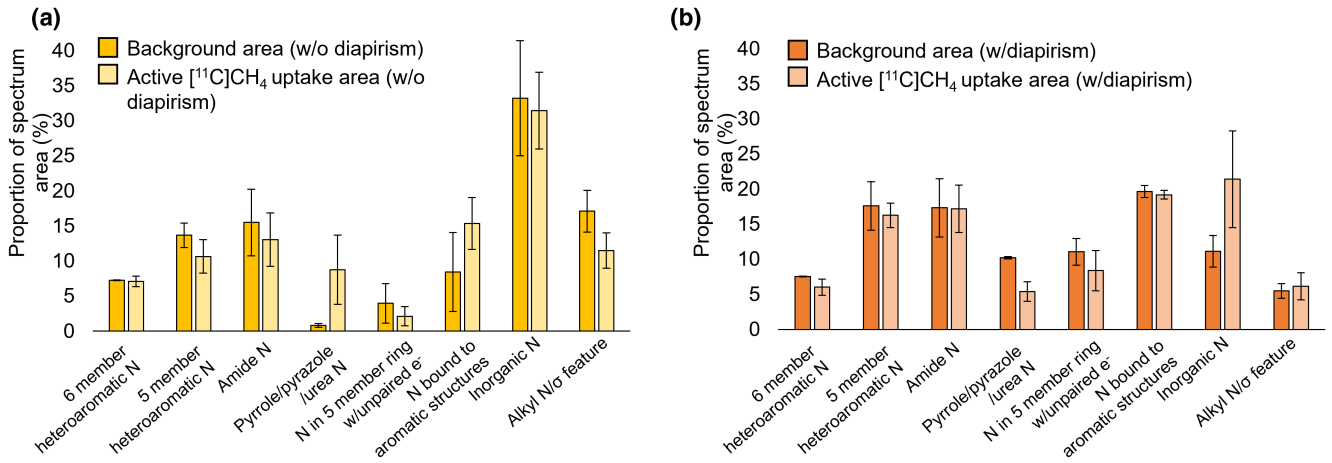

FIGURE 4 Averaged N-XANES speciation results with comparisons between soil aliquots: (a) background ($n = 2$) and active ($n = 4$) regions on non-diapiric soils and b) background ($n = 2$) and active ($n = 4$) regions on diapiric soils. Error bars for both plots represent standard errors of averaged values

No other methane monoxygenases were present in the filtered dataset. In contrast, downstream formaldehyde assimilation into formate, ribulose monophosphate (RuMP), serine, and tricarboxylic acid (TCA) cycle fluxes, as well as cyanate-carbamate and glutamate synthase (GOGAT) N metabolism fluxes were consistently present and enriched in [^{11}C]CH_4 uptake hotspots (Figure 6; Kanehisa, 2000).

Although no CH_4 metabolism-related genes enriched in [^{11}C]CH_4 uptake hotspots directly encode for inorganic N transporters, there are connections between specific CH_4-related metabolic pathways in *R. pickettii* and inorganic N. For example, GOGAT pathway genes, a possible pathway for microbial ammonium incorporation into amino acids (Geisseler et al., 2010), are enriched in *R. pickettii* within active zones of CH_4 uptake. Enrichment of another N-related metabolic

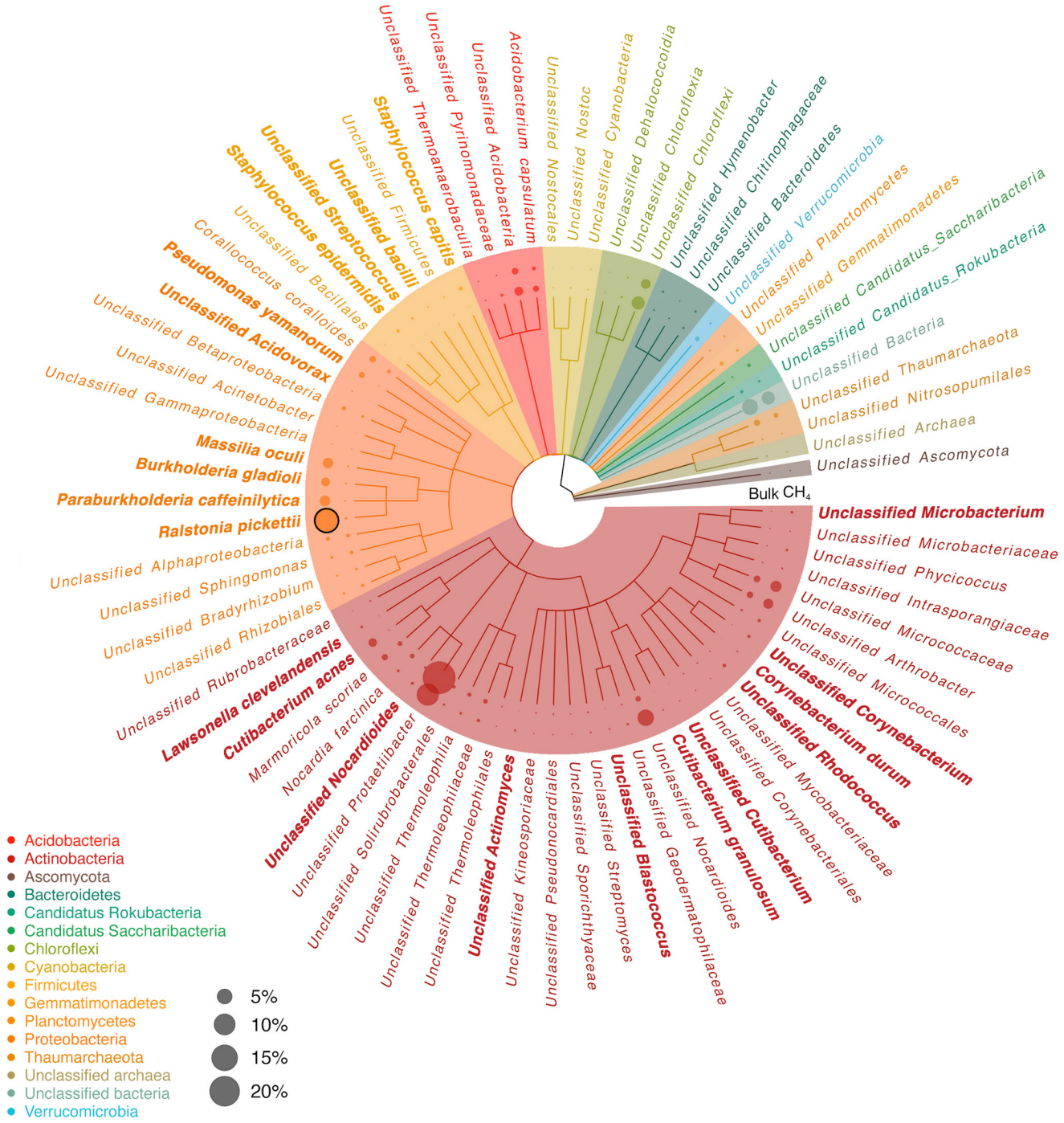

FIGURE 5 Taxonomy and relative abundances of the desert soil microbial communities. The tree represents a radial taxonomy of the 76 unique archeal ($n = 3$), bacterial ($n = 72$), and fungal ($n = 1$) taxa. Taxa labelled in bold were >10-fold more abundant in $[^{11}C]CH_4$ hotspots relative to background (bulk) soil. *Ralstonia pickettii* relative abundance is highlighted

gene was notably observed in *R. pickettii* within active $[^{11}C]CH_4$ uptake regions. The gene coding for cyanate lyase was also enriched in $[^{11}C]CH_4$ uptake hotspots. Cyanate lyase catalyses cyanate transformation to carbamate, which may convert to NH_3 and CO_2 (Johnson & Anderson, 1987; Mooshammer et al., 2021). While this may be an important NH_3 source for microorganisms, low concentrations of cyanate (≈pmol g^{-1} soil) and its transient nature (Mooshammer et al., 2021) preclude use of N-XANES for identification in soils.

4 | DISCUSSION

4.1 | Radioisotope imaging bridges the gap between metagenomic and chemical speciation in CH_4 uptake hotspots

Our C XANES spectroscopic results contrast with previous spectroscopic characterization of SOC in Arctic desert frost

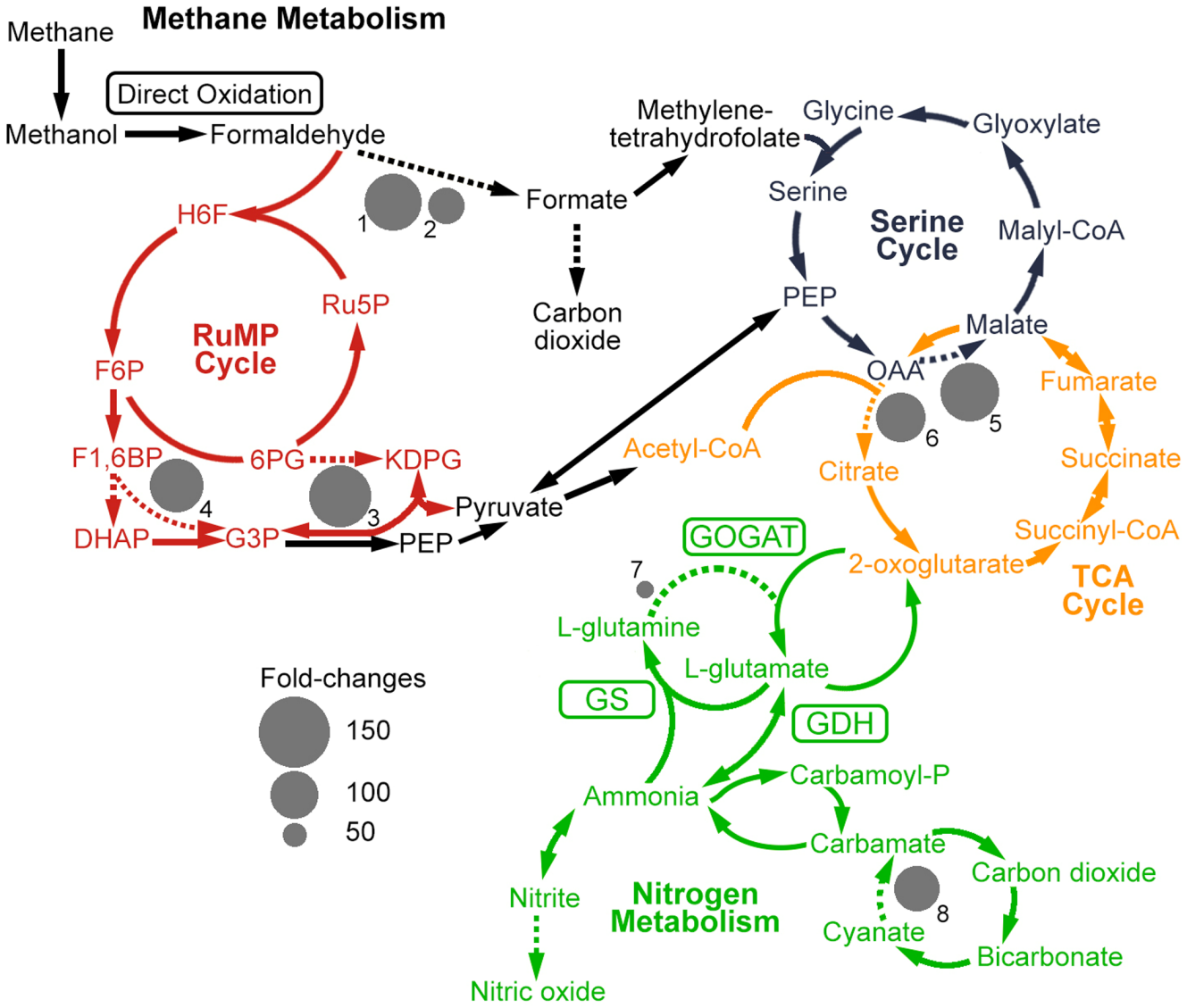

FIGURE 6 Simplified pathways for methane and nitrogen metabolism in *Ralstonia pickettii*. Grey circles indicate significant fold-changes in KEGG function gene abundance from background to methane hotspots determined through autoradiographic analysis of High Arctic soils. Dashed lines specify which pathways correspond to the fold-changes. Methane/carbon metabolism pathways and genes are as follows: 1. S-formylglutathione hydrolase [EC:3.1.2.12], frmB, ESD, fghA. 2. S-(hydroxymethyl)glutathione dehydrogenase [EC.1.1.1.284], frmA, ADH5, adhC. 3. Phosphogluconate dehydratase [EC:4.2.1.12], edd. 4. Fructose-bisphosphate aldolase, class II [EC:4.1.2.13], FBA, fbaA. 5. Malate dehydrogenase [EC:1.1.1.37], mdh. 6. Citrate synthase [EC:2.3.3.1], CS, gltA. Nitrogen metabolism pathways and genes: 7. Glutamate synthase (NADPH) large chain [EC:1.4.1.13], gltB. 8. Cyanate lyase [EC:4.2.1.104], cynS. RuMP, ribulose monophosphate cycle. Ammonium assimilation pathways: GDH, glutamate dehydrogenase; GOGAT, glutamine 2-oxoglutarate amidotransferase; GS, glutamine synthetase

boils, which showed relative enrichment of polysaccharide and aromatic-rich SOC constituents in diapiric frost boils (Ota et al., 2020). SOC speciation is similar within active [^{11}C]CH_4 uptake regions compared with background regions, even under more constrained comparison (Figure S5b), indicating SOC speciation does not spatially relate with CH_4 uptake across these Arctic desert soils at spatial scales probed, regardless of diapirism (Figure S5c). While not previously studied, N XANES speciation of diapiric and non-diapiric frost boils is consistent with diapiric translocation. These processes transfer dissolved organic species upward into soils, lowering inorganic N proportionally in regions of diapiric influence. These results indicate soil N species may be more transformation-prone than C in these soils. It is also conceivable that N-XANES spectroscopy is more sensitive to differences in speciation relative to C-XANES spectroscopy.

The greater relative proportion of inorganic N species in active CH_4 uptake regions in diapiric frost boils reflects previously described links between methane oxidation and inorganic N species in soils. Inorganic N species are a key methanotrophic activity modulator with soil CH_4 uptake enhanced by increased inorganic N in

N-limited environments (Bodelier & Laanbroek, 2004; Mohanty et al., 2006). Suppression, however, may be linked to NH_4^+ competition with CH_4 for active sites on methane monooxygenase enzymes, which catalyze NH_3 oxidation (Bodelier & Laanbroek, 2004). Furthermore, methanotrophic NH_3 oxidation may form toxic compounds, including hydroxylamine and nitrite (Bodelier & Laanbroek, 2004). A spatial relationship between active CH_4 uptake and inorganic N species indicates that enhancement of methanotrophic activity, rather than suppression, may have a greater influence in diapiric frost boils. Given the implications of diapirism for soil C/N biogeochemistry (i.e., greater SOC and nutrient concentrations) and previous results linking SOC composition with GHG fluxes in cryoturbic Arctic soils, the spatial association between active CH_4 uptake and higher inorganic N proportion is counter to our hypotheses that a diapirism-induced link between C speciation and active CH_4 oxidation would be observed.

Despite indications that *R. pickettii* was involved in CH_4 uptake by these soils, we found no previous studies describing *R. pickettii* as part of active CH_4 cycling in soils. *Ralstonia* represents a diverse genus of Proteobacteria found widely in soils, waters, and sediments. *Ralstonia* have been tentatively connected with CH_4 oxidation in sub-Arctic lake sediments (Martinez-Cruz et al., 2017). Furthermore, CH_4 metabolism-related functions were identified in methylotrophic *Ralstonia* species and taxonomic groups formerly associated with the *Ralstonia* genus (Doronina et al., 2001; Friedebold & Bowien, 1993; Habibi & Vahabzadeh, 2013; Miyake-Nakayama et al., 2006). These previous studies indicate a relationship between *R. pickettii* is conceivable, albeit tentative. This suggests the role of *R. pickettii* in soil CH_4 cycling, particularly Arctic soils, may warrant further investigation Our findings here coupled with those of previous studies, suggest that the dynamics of high-affinity methanotrophs found in mineral cryosols are likely very different from the low-affinity methanotrophy that occurs in high-methane environments like peatlands (Rusley et al., 2019).

Functional characteristics of *R. pickettii* within active uptake CH_4 regions relate well to N-XANES speciation. Enrichment of GOGAT pathway genes, versus gene enrichment directly related to the lower-affinity, less costly, glutamate dehydrogenase pathway (Geisseler et al., 2010), aligns with low nutrient status in these Arctic desert soils. In low nutrient availability soils, the energetic trade-off of higher-affinity N acquisition strategies is conceivable and highlights N availability influence on microbial dynamics in Arctic desert soils. This corresponds with localized N-XANES speciation, which showed a spatial preference for active CH_4 uptake in regions of greater inorganic N proportion on diapiric frost boils.

4.2 | Implications for findings and methodology

We demonstrate that diapiric features in Arctic desert frost boils impose spatial relationships between CH_4 uptake and inorganic N species not observed in non-diapiric soils. This observation, coupled with high-affinity NH_4^+ assimilation gene enrichment in a *Ralstonia* species within CH_4 uptake hotspots, provides evidence for the disputed positive relationship between inorganic N and soil CH_4 oxidation (Bodelier & Laanbroek, 2004). Metagenomic results inform ecology of Arctic CH_4 cycling by connecting soil CH_4 uptake with *R. Pickettii*, despite possessing an incomplete CH_4 metabolism pathway. These results contrast with our hypothesis that CH_4 oxidation would spatially associate with distinct C species previously related to GHG dynamics in cryodisturbed Arctic soils.

Our work highlights the relationship between pedogenic cryoturbation processes and how these soil properties mediate biogeochemical drivers of GHG fluxes in Arctic desert soils. These interactions are particularly important as Arctic deserts are expected to serve as an increasingly large CH_4 sink with Arctic temperature increases and because cryoturbic features are anticipated to become more prevalent with more frequent freeze-thaw cycles (Klaus et al., 2013). Coupled with an expected increase of terrestrial N in the Arctic under future climate scenarios, either by enhanced biological N_2 fixation with higher temperatures (Chapin et al., 1992) or increasing extreme precipitation events over the Arctic leading to greater atmospheric N deposition (Choudhary et al., 2016; Kühnel et al., 2011), interactive N, and GHG dynamics within cryoturbic soils may be a critical factor for future predictions of Arctic soil C cycling.

We can now visualize and isolate regions of biogeochemical activity in soils for subsequent metagenomic and spectroscopic characterization using a novel radiotracer, XANES, and metagenomic approach. This framework probes convergent spatial relationships between active CH_4 uptake and localized microbiological/chemical speciation, yielding new insights into GHG cycling in Arctic desert soils. With the range of positron-emitting radionuclides/chemistries available at production facilities worldwide (see IAEA.org; Database of Cyclotrons for Radionuclide Production), imaging technologies (e.g., autoradiography, positron emission tomography), and flexible interface with complimentary analyses, this approach is generally applicable to many biotic processes within the context of global change. Plant or soil dosing with other available radiotracers (e.g., $[^{11}C]CO_2$, $[^{11}C]$-sugars, $[^{13}N]N_2$, $[^{13}N]\ NO_3^-$, $[^{13}N]\ N_2O$) makes studies on other critical processes related to GHG dynamics accessible (e.g., respiration, C/N-fixation, denitrification; Schmidt et al., 2020). With respect to approaches employed here, X-ray absorption techniques are available at synchrotron facilities worldwide and provide chemical speciation for elements involved, directly or peripherally, in these processes. Furthermore, short radionuclide half-lives make repeated dosing and imaging of a single sample or subject under manipulated environmental conditions possible, serving as a powerful tool for probing biological responses to a changing climate.

ACKNOWLEDGMENTS

M.P.S. acknowledges the NSERC CREATE-SAFER program, an Engineering Research Council Collaborative Research and Development grant supported by Federated Cooperatives Limited

(Grant no. 537285-18), and the Sylvia Fedoruk Canadian Centre for Nuclear Innovation (Grant no. J2018-0041) for support. Drs. Jay Dynes and Zachary Arthur of the Canadian Light Source and Ruan Firmano of University of São Paulo assisted in the collection of XANES data. The findings and conclusions in this publication are those of the author(s) and should not be construed to represent any official USDA or U.S. Government determination or policy. Mention of trade names or commercial products in this publication is solely for the purpose of providing specific information and does not imply recommendation or endorsement by the U.S. Department of Agriculture. Research described in this paper was performed at the Canadian Light Source (CLS), which is supported by the Canada Foundation for Innovation, Natural Sciences and Engineering Research Council of Canada, the University of Saskatchewan, the Government of Saskatchewan, Western Economic Diversification Canada, the National Research Council Canada, and the Canadian Institutes of Health Research.

CONFLICT OF INTEREST

The authors declare no conflicting interests.

AUTHOR CONTRIBUTIONS

M.P.S.—Study design, collection, and analysis of radiochemistry and XANES data, writing original manuscript, writing revised manuscript; S.D.M.—Study design, metagenomic analyses, processing radiochemistry data, writing original manuscript, editing revised manuscript; C.S.—Constructed radioisotope purification and synthesis system, performed radiographic imaging; A.S.—Grew model organism, collection of radiochemistry data, edited original manuscript; M.O.—Collection of field soils, bulk soil characterization, edited original manuscript; T.W.T.—Soil preparation, soil incubation; U.A.—Metagenomic analyses; L.Y.S.—Metagenomic analyses, writing original manuscript, editing revised manuscript; T.R.—Collection of XANES data, editing original manuscript; K.S.—Metagenomic analyses, editing original manuscript; D.P.—Study design, funding acquisition, collection, and analysis of XANES data; S.D.S.—Study design, funding acquisition, writing original manuscript, manuscript revisions.

DATA AVAILABILITY STATEMENT

The spectroscopic and metagenomic data that support the findings of this study are openly available through datadryad.org (https://doi.org/10.5061/dryad.jwstqjqbs).

ORCID

Michael P. Schmidt https://orcid.org/0000-0001-8789-9204
Steven D. Mamet https://orcid.org/0000-0002-3510-3814
Curtis Senger https://orcid.org/0000-0002-1891-4965
Mitsuaki Ota https://orcid.org/0000-0002-8326-2334
Lisa Y. Stein https://orcid.org/0000-0001-5095-5022
Tom Regier https://orcid.org/0000-0002-0022-3509
Derek Peak https://orcid.org/0000-0002-8876-3605
Steven D. Siciliano https://orcid.org/0000-0002-8994-3341

REFERENCES

Abràmoff, M., Magalhães, P., & Ram, S. (2004). Image Processing with ImageJ. *Biophotonics International*, *11*, 36–42.

Allen, H. K., Bayles, D. O., Looft, T., Trachsel, J., Bass, B. E., Alt, D. P., Bearson, S. M. D., Nicholson, T., & Casey, T. A. (2016). Pipeline for amplifying and analyzing amplicons of the V1–V3 region of the 16S rRNA gene. *BMC Research Notes*, *9*(1), 380. https://doi.org/10.1186/s13104-016-2172-6

Baani, M., & Liesack, W. (2008). Two isozymes of particulate methane monooxygenase with different methane oxidation kinetics are found in *Methylocystis* sp. Strain SC2. *Proceedings of the National Academy of Sciences of the United States of America*, *105*(29), 10203–10208. https://doi.org/10.1073/pnas.0702643105

Baveye, P. C., Otten, W., Kravchenko, A., Balseiro-Romero, M., Beckers, É., Chalhoub, M., Darnault, C., Eickhorst, T., Garnier, P., Hapca, S., Kiranyaz, S., Monga, O., Mueller, C. W., Nunan, N., Pot, V., Schlüter, S., Schmidt, H., & Vogel, H.-J. (2018). Emergent properties of microbial activity in heterogeneous soil microenvironments: Different research approaches are slowly converging, yet major challenges remain. *Frontiers in Microbiology*, *9*, 1929. https://doi.org/10.3389/fmicb.2018.01929

Biskaborn, B. K., Smith, S. L., Noetzli, J., Matthes, H., Vieira, G., Streletskiy, D. A., Schoeneich, P., Romanovsky, V. E., Lewkowicz, A. G., Abramov, A., Allard, M., Boike, J., Cable, W. L., Christiansen, H. H., Delaloye, R., Diekmann, B., Drozdov, D., Etzelmüller, B., Grosse, G., … Lantuit, H. (2019). Permafrost is warming at a global scale. *Nature Communications*, *10*(1), 264. https://doi.org/10.1038/s41467-018-08240-4

Bliss, L. C., Henry, G. H. R., Svoboda, J., & Bliss, D. I. (1994). Patterns of plant distribution within two polar desert landscapes. *Arctic and Alpine Research*, *26*(1), 46–55. https://doi.org/10.1080/00040851.1994.12003038

Bodelier, P. L. E., & Laanbroek, H. J. (2004). Nitrogen as a regulatory factor of methane oxidation in soils and sediments. *FEMS Microbiology Ecology*, *47*(3), 265–277. https://doi.org/10.1016/S0168-6496(03)00304-0

Brummell, M. E., Farrell, R. E., & Siciliano, S. D. (2012). Greenhouse gas soil production and surface fluxes at a high arctic polar oasis. *Soil Biology and Biochemistry*, *52*, 1–12. https://doi.org/10.1016/j.soilbio.2012.03.019

Brummell, M. E., Guy, A., & Siciliano, S. D. (2015). Does diapirism influence greenhouse gas production on patterned ground in the high arctic? *Soil Science Society of America Journal*, *79*(3), 889–895. https://doi.org/10.2136/sssaj2015.01.0026

Buchfink, B., Xie, C., & Huson, D. H. (2015). Fast and sensitive protein alignment using DIAMOND. *Nature Methods*, *12*(1), 59–60. https://doi.org/10.1038/nmeth.3176

Canadian Agricultural Services Coordinating Committee, National Research Council Canada, & Canada (Eds.). (1998). *The Canadian system of soil classification* (3rd ed.). NRC Research Press.

Chapin, F. L., Jefferies, R. L., Reynolds, J. F., Shaver, G. R., & Svoboda, J. (Eds.). (1992). *Arctic ecosystems in a changing climate*. Academic Press. https://doi.org/10.1016/C2009-0-02634-8

Choudhary, S., Blaud, A., Osborn, A. M., Press, M. C., & Phoenix, G. K. (2016). Nitrogen accumulation and partitioning in a high arctic tundra ecosystem from extreme atmospheric N deposition events. *Science of the Total Environment*, *554–555*, 303–310. https://doi.org/10.1016/j.scitotenv.2016.02.155

Clark, K., Karsch-Mizrachi, I., Lipman, D. J., Ostell, J., & Sayers, E. W. (2016). GenBank. *Nucleic Acids Research*, *44*(D1), D67–D72. https://doi.org/10.1093/nar/gkv1276

Curry, C. L. (2009). The consumption of atmospheric methane by soil in a simulated future climate. *Biogeosciences*, *6*(11), 2355–2367. https://doi.org/10.5194/bg-6-2355-2009

Dhillon, G. S., Gillespie, A., Peak, D., & Van Rees, K. C. J. (2017). Spectroscopic investigation of soil organic matter composition for

shelterbelt agroforestry systems. *Geoderma*, *298*, 1–13. https://doi.org/10.1016/j.geoderma.2017.03.016

Doronina, N. V., Darmaeva, T. D., & Trotsenko, Y. A. (2001). Novel aerobic methylotrophic isolates from the soda lakes of the southern Transbaikal region. *Microbiology*, *70*(3), 342–348. https://doi.org/10.1023/A:1010415730337

Dynes, J. J., Regier, T. Z., Snape, I., Siciliano, S. D., & Peak, D. (2015). Validating the scalability of soft X-ray spectromicroscopy for quantitative soil ecology and biogeochemistry research. *Environmental Science & Technology*, *49*(2), 1035–1042. https://doi.org/10.1021/es505271p

Emmerton, C. A., St. Louis, V. L., Lehnherr, I., Humphreys, E. R., Rydz, E., & Kosolofski, H. R. (2014). The net exchange of methane with high Arctic landscapes during the summer growing season. *Biogeosciences*, *11*(12), 3095–3106. https://doi.org/10.5194/bg-11-3095-2014

Food and Agriculture Organization of the United Nations. (2014). *World reference base for soil resources 2014: International soil classification system for naming soils and creating legends for soil maps*. FAO. http://www.fao.org/3/i3794en/I3794en.pdf

Friedebold, J., & Bowien, B. (1993). Physiological and biochemical characterization of the soluble formate dehydrogenase, a molybdoenzyme from *Alcaligenes eutrophus*. *Journal of Bacteriology*, *175*(15), 4719–4728. https://doi.org/10.1128/JB.175.15.4719-4728.1993

Geisseler, D., Horwath, W. R., Joergensen, R. G., & Ludwig, B. (2010). Pathways of nitrogen utilization by soil microorganisms—A review. *Soil Biology and Biochemistry*, *42*(12), 2058–2067. https://doi.org/10.1016/j.soilbio.2010.08.021

Gillespie, A. W., Phillips, C. L., Dynes, J. J., Chevrier, D., Regier, T. Z., & Peak, D. (2015). Advances in using soft X-ray spectroscopy for measurement of soil biogeochemical processes. In *Advances in agronomy* (Vol. *133*, pp. 1–32). Elsevier. https://doi.org/10.1016/bs.agron.2015.05.003

Gillespie, A. W., Sanei, H., Diochon, A., Ellert, B. H., Regier, T. Z., Chevrier, D., Dynes, J. J., Tarnocai, C., & Gregorich, E. G. (2014). Perennially and annually frozen soil carbon differ in their susceptibility to decomposition: Analysis of Subarctic earth hummocks by bioassay, XANES and pyrolysis. *Soil Biology and Biochemistry*, *68*, 106–116. https://doi.org/10.1016/j.soilbio.2013.09.021

Gillespie, A. W., Walley, F. L., Farrell, R. E., Leinweber, P., Eckhardt, K.-U., Regier, T. Z., & Blyth, R. I. R. (2011). XANES and pyrolysis-fims evidence of organic matter composition in a hummocky landscape. *Soil Science Society of America Journal*, *75*(5), 1741–1755. https://doi.org/10.2136/sssaj2010.0279

Gray, N. D., McCann, C. M., Christgen, B., Ahammad, S. Z., Roberts, J. A., & Graham, D. W. (2014). Soil geochemistry confines microbial abundances across an arctic landscape; implications for net carbon exchange with the atmosphere. *Biogeochemistry*, *120*(1–3), 307–317. https://doi.org/10.1007/s10533-014-9997-7

Guy, A. L., Siciliano, S. D., & Lamb, E. G. (2015). Spiking regional vis-NIR calibration models with local samples to predict soil organic carbon in two High Arctic polar deserts using a vis-NIR probe. *Canadian Journal of Soil Science*, *95*(3), 237–249. https://doi.org/10.4141/cjss-2015-004

Habibi, A., & Vahabzadeh, F. (2013). Degradation of formaldehyde at high concentrations by phenol-adapted *Ralstonia eutropha* closely related to pink-pigmented facultative methylotrophs. *Journal of Environmental Science and Health, Part A*, *48*(3), 279–292. https://doi.org/10.1080/10934529.2013.726829

Holmes, A. J., Roslev, P., McDonald, I. R., Iversen, N., Henriksen, K., & Murrell, J. C. (1999). Characterization of methanotrophic bacterial populations in soils showing atmospheric methane uptake. *Applied and Environmental Microbiology*, *65*(8), 3312–3318. https://doi.org/10.1128/AEM.65.8.3312-3318.1999

Hua, Z.-S., Wang, Y.-L., Evans, P. N., Qu, Y.-N., Goh, K. M., Rao, Y.-Z., Qi, Y.-L., Li, Y.-X., Huang, M.-J., Jiao, J.-Y., Chen, Y.-T., Mao, Y.-P., Shu, W.-S., Hozzein, W., Hedlund, B. P., Tyson, G. W., Zhang, T., & Li, W.-J. (2019). Insights into the ecological roles and evolution of methyl-coenzyme M reductase-containing hot spring Archaea. *Nature Communications*, *10*(1), 4574. https://doi.org/10.1038/s41467-019-12574-y

Huson, D. H., Auch, A. F., Qi, J., & Schuster, S. C. (2007). MEGAN analysis of metagenomic data. *Genome Research*, *17*(3), 377–386. https://doi.org/10.1101/gr.5969107

Irvin, B. J., Ventura, S. J., & Slater, B. K. (1997). Fuzzy and isodata classification of landform elements from digital terrain data in Pleasant Valley, Wisconsin. *Geoderma*, *77*(2–4), 137–154. https://doi.org/10.1016/S0016-7061(97)00019-0

Johnson, W. V., & Anderson, P. M. (1987). Bicarbonate is a recycling substrate for cyanase. *Journal of Biological Chemistry*, *262*(19), 9021–9025. https://doi.org/10.1016/S0021-9258(18)48040-4

Juncher Jørgensen, C., Lund Johansen, K. M., Westergaard-Nielsen, A., & Elberling, B. (2015). Net regional methane sink in High Arctic soils of northeast Greenland. *Nature Geoscience*, *8*(1), 20–23. https://doi.org/10.1038/ngeo2305

Kanehisa, M. (2000). KEGG: Kyoto encyclopedia of genes and genomes. *Nucleic Acids Research*, *28*(1), 27–30. https://doi.org/10.1093/nar/28.1.27

Kinsella, K., Schlyer, D. J., Fowler, J. S., Martinez, R. J., & Sobecky, P. A. (2012). Evaluation of positron emission tomography as a method to visualize subsurface microbial processes. *Journal of Hazardous Materials*, *213–214*, 498–501. https://doi.org/10.1016/j.jhazmat.2012.01.037

Klaus, M., Becher, M., & Klaminder, J. (2013). Cryogenic soil activity along bioclimatic gradients in Northern Sweden: Insights from eight different proxies: Cryogenic soil activity along bioclimatic gradients. *Permafrost and Periglacial Processes*, *24*(3), 210–223. https://doi.org/10.1002/ppp.1778

Knapp, C. W., Fowle, D. A., Kulczycki, E., Roberts, J. A., & Graham, D. W. (2007). Methane monooxygenase gene expression mediated by methanobactin in the presence of mineral copper sources. *Proceedings of the National Academy of Sciences of the United States of America*, *104*(29), 12040–12045. https://doi.org/10.1073/pnas.0702879104

Kühnel, R., Roberts, T. J., Björkman, M. P., Isaksson, E., Aas, W., Holmén, K., & Ström, J. (2011). 20-year climatology of NO_3^- and NH_4^+ wet deposition at Ny-Ålesund, Svalbard. *Advances in Meteorology*, *2011*, 1–10. https://doi.org/10.1155/2011/406508

L'Annunziata, M. (2012). Radiation physics and radionuclide decay. In M. F. L'Annunziata (Ed.), *Handbook of radioactivity analysis* (3rd ed., pp. 1–162). Elsevier.

Lau, M. C. Y., Stackhouse, B. T., Layton, A. C., Chauhan, A., Vishnivetskaya, T. A., Chourey, K., Ronholm, J., Mykytczuk, N. C. S., Bennett, P. C., Lamarche-Gagnon, G., Burton, N., Pollard, W. H., Omelon, C. R., Medvigy, D. M., Hettich, R. L., Pfiffner, S. M., Whyte, L. G., & Onstott, T. C. (2015). An active atmospheric methane sink in high Arctic mineral cryosols. *The ISME Journal*, *9*(8), 1880–1891. https://doi.org/10.1038/ismej.2015.13

Leinweber, P., Kruse, J., Walley, F. L., Gillespie, A., Eckhardt, K.-U., Blyth, R. I. R., & Regier, T. (2007). Nitrogen *K*-edge XANES—An overview of reference compounds used to identify unknown' organic nitrogen in environmental samples. *Journal of Synchrotron Radiation*, *14*(6), 500–511. https://doi.org/10.1107/S0909049507042513

Li, D., Liu, C.-M., Luo, R., Sadakane, K., & Lam, T.-W. (2015). MEGAHIT: An ultra-fast single-node solution for large and complex metagenomics assembly via succinct de Bruijn graph. *Bioinformatics*, *31*(10), 1674–1676. https://doi.org/10.1093/bioinformatics/btv033

Linstrom, P. (1997). *NIST chemistry WebBook, NIST standard reference database 69*. National Institute of Standards and Technology. https://doi.org/10.18434/T4D303

Mamet, S. D., Helgason, B. L., Lamb, E. G., McGillivray, A., Stanley, K. G., Robinson, S. J., Aziz, S. U., Vail, S., & Siciliano, S. D. (2021).

Phenology-dependent root bacteria enhance yield of Brassica napus. *Soil Biology and Biochemistry*, 108468. https://doi.org/10.1016/j.soilbio.2021.108468

Martinez-Cruz, K., Leewis, M.-C., Herriott, I. C., Sepulveda-Jauregui, A., Anthony, K. W., Thalasso, F., & Leigh, M. B. (2017). Anaerobic oxidation of methane by aerobic methanotrophs in sub-Arctic lake sediments. *Science of the Total Environment*, *607–608*, 23–31. https://doi.org/10.1016/j.scitotenv.2017.06.187

Miyake-Nakayama, C., Ikatsu, H., Kashihara, M., Tanaka, M., Arita, M., Miyoshi, S., & Shinoda, S. (2006). Biodegradation of dichloromethane by the polyvinyl alcohol-immobilized methylotrophic bacterium *Ralstonia metallidurans* PD11. *Applied Microbiology and Biotechnology*, *70*(5), 625–630. https://doi.org/10.1007/s00253-005-0194-4

Mohanty, S. R., Bodelier, P. L. E., Floris, V., & Conrad, R. (2006). Differential effects of nitrogenous fertilizers on methane-consuming microbes in rice field and forest soils. *Applied and Environmental Microbiology*, *72*(2), 1346–1354. https://doi.org/10.1128/AEM.72.2.1346-1354.2006

Mooshammer, M., Wanek, W., Jones, S. H., Richter, A., & Wagner, M. (2021). Cyanate is a low abundant but actively cycled nitrogen compound in soil. *Communications Earth & Environment*, *2*, 161. https://doi.org/10.1101/2020.07.12.199737

Muller, A. L., Hardy, S. P., Mamet, S. D., Ota, M., Lamb, E. G., & Siciliano, S. D. (2017). *Salix arctica* changes root distribution and nutrient uptake in response to subsurface nutrients in High Arctic deserts. *Ecology*, *98*(8), 2158–2169. https://doi.org/10.1002/ecy.1908

Muller, A., Lamb, E. G., & Siciliano, S. D. (2022). The silent carbon pool: Cryoturbic enriched organic matter in Canadian High Arctic semi-deserts. *Geoderma*, *415*, 115781. https://doi.org/10.1016/j.geoderma.2022.115781

Myneni, S. C. B. (2002). Soft X-ray spectroscopy and spectromicroscopy studies of organic molecules in the environment. *Reviews in Mineralogy and Geochemistry*, *49*(1), 485–579. https://doi.org/10.2138/gsrmg.49.1.485

Oh, Y., Zhuang, Q., Liu, L., Welp, L. R., Lau, M. C. Y., Onstott, T. C., Medvigy, D., Bruhwiler, L., Dlugokencky, E. J., Hugelius, G., D'Imperio, L., & Elberling, B. (2020). Reduced net methane emissions due to microbial methane oxidation in a warmer Arctic. *Nature Climate Change*, *10*(4), 317–321. https://doi.org/10.1038/s41558-020-0734-z

Ota, M. (2021). *Biogeochemical and ecological responses to warming climate in High Arctic polar deserts*. University of Saskatchewan.

Ota, M., Mamet, S. D., Muller, A. L., Lamb, E. G., Dhillon, G., Peak, D., & Siciliano, S. D. (2020). Could cryoturbic diapirs be key for understanding ecological feedbacks to climate change in high arctic polar deserts? *Journal of Geophysical Research: Biogeosciences*, *125*(3). https://doi.org/10.1029/2019JG005263

Paradis, E., & Schliep, K. (2019). ape 5.0: An environment for modern phylogenetics and evolutionary analyses in R. *Bioinformatics*, *35*(3), 526–528. https://doi.org/10.1093/bioinformatics/bty633

Perryman, C. R., McCalley, C. K., Malhotra, A., Fahnestock, M. F., Kashi, N. N., Bryce, J. G., Giesler, R., & Varner, R. K. (2020). Thaw transitions and redox conditions drive methane oxidation in a permafrost Peatland. *Journal of Geophysical Research: Biogeosciences*, *125*(3). https://doi.org/10.1029/2019JG005526

Qin, W., Zheng, Y., Zhao, F., Wang, Y., Urakawa, H., Martens-Habbena, W., Liu, H., Huang, X., Zhang, X., Nakagawa, T., Mende, D. R., Bollmann, A., Wang, B., Zhang, Y., Amin, S. A., Nielsen, J. L., Mori, K., Takahashi, R., Virginia Armbrust, E., … Ingalls, A. E. (2020). Alternative strategies of nutrient acquisition and energy conservation map to the biogeography of marine ammonia-oxidizing archaea. *The ISME Journal*, *14*(10), 2595–2609. https://doi.org/10.1038/s41396-020-0710-7

Ravel, B., & Newville, M. (2005). ATHENA, ARTEMIS, HEPHAESTUS: Data analysis for X-ray absorption spectroscopy using IFEFFIT. *Journal of Synchrotron Radiation*, *12*(4), 537–541. https://doi.org/10.1107/S0909049505012719

Rusley, C., Onstott, T. C., Vishnivetskaya, T. A., Layton, A., Chauhan, A., Pfiffner, S. M., Whyte, L. G., & Lau, M. C. Y. (2019). Metagenome-assembled genome of USCα AHI, a potential high-affinity methanotroph from Axel Heiberg Island, Canadian High Arctic. *Microbiology Resource Announcements*, *8*(46), e01178–e1219. https://doi.org/10.1128/MRA.01178-19

Schimel, J. P., & Schaeffer, S. M. (2012). Microbial control over carbon cycling in soil. *Frontiers in Microbiology*, *3*. https://doi.org/10.3389/fmicb.2012.00348

Schindelin, J., Arganda-Carreras, I., Frise, E., Kaynig, V., Longair, M., Pietzsch, T., Preibisch, S., Rueden, C., Saalfeld, S., Schmid, B., Tinevez, J.-Y., White, D. J., Hartenstein, V., Eliceiri, K., Tomancak, P., & Cardona, A. (2012). Fiji: An open-source platform for biological-image analysis. *Nature Methods*, *9*(7), 676–682. https://doi.org/10.1038/nmeth.2019

Schmidt, M. P., Mamet, S. D., Ferrieri, R. A., Peak, D., & Siciliano, S. D. (2020). From the outside in: An overview of positron imaging of plant and soil processes. *Molecular Imaging*, *19*, 153601212096640. https://doi.org/10.1177/1536012120966405

Schuur, E. A. G., & Abbott, B. (2011). High risk of permafrost thaw. *Nature*, *480*(7375), 32–33. https://doi.org/10.1038/480032a

Schuur, E. A. G., Abbott, B. W., Bowden, W. B., Brovkin, V., Camill, P., Canadell, J. G., Chanton, J. P., Chapin, F. S., Christensen, T. R., Ciais, P., Crosby, B. T., Czimczik, C. I., Grosse, G., Harden, J., Hayes, D. J., Hugelius, G., Jastrow, J. D., Jones, J. B., Kleinen, T., … Zimov, S. A. (2013). Expert assessment of vulnerability of permafrost carbon to climate change. *Climatic Change*, *119*(2), 359–374. https://doi.org/10.1007/s10584-013-0730-7

Schuur, E. A. G., McGuire, A. D., Schädel, C., Grosse, G., Harden, J. W., Hayes, D. J., Hugelius, G., Koven, C. D., Kuhry, P., Lawrence, D. M., Natali, S. M., Olefeldt, D., Romanovsky, V. E., Schaefer, K., Turetsky, M. R., Treat, C. C., & Vonk, J. E. (2015). Climate change and the permafrost carbon feedback. *Nature*, *520*(7546), 171–179. https://doi.org/10.1038/nature14338

Sullivan, B. W., Selmants, P. C., & Hart, S. C. (2013). Does dissolved organic carbon regulate biological methane oxidation in semi-arid soils? *Global Change Biology*, *19*(7), 2149–2157. https://doi.org/10.1111/gcb.12201

Tamames, J., & Puente-Sánchez, F. (2019). SqueezeMeta, a highly portable, fully automatic metagenomic analysis pipeline. *Frontiers in Microbiology*, *9*, 3349. https://doi.org/10.3389/fmicb.2018.03349

Tatusov, R. L., Fedorova, N. D., Jackson, J. D., Jacobs, A. R., Kiryutin, B., Koonin, E. V., Krylov, D. M., Mazumder, R., Mekhedov, S. L., Nikolskaya, A. N., Rao, B. S., Smirnov, S., Sverdlov, A. V., Vasudevan, S., Wolf, Y. I., Yin, J. J., & Natale, D. A. (2003). The COG database: An updated version includes eukaryotes. *BMC Bioinformatics*, *4*(1), 41. https://doi.org/10.1186/1471-2105-4-41

Tewson, T. J., Banks, W., Franceschini, M., & Hoffpauir, J. (1989). A trap for the removal of nitrogen oxides from carbon-11 carbon dioxide. *International Journal of Radiation Applications and Instrumentation. Part A. Applied Radiation and Isotopes*, *40*(9), 765–768. https://doi.org/10.1016/0883-2889(89)90094-4

Thorpe, C. L., Williams, H. A., Boothman, C., Lloyd, J. R., & Morris, K. (2019). Positron emission tomography to visualise in-situ microbial metabolism in natural sediments. *Applied Radiation and Isotopes*, *144*, 104–110. https://doi.org/10.1016/j.apradiso.2018.11.005

Tou, J. T., & Gonzalez, R. C. (1974). *Pattern recognition principles*. Addison-Wesley Pub. Co.

Tveit, A. T., Hestnes, A. G., Robinson, S. L., Schintlmeister, A., Dedysh, S. N., Jehmlich, N., von Bergen, M., Herbold, C., Wagner, M., Richter, A., & Svenning, M. M. (2019). Widespread soil bacterium that oxidizes atmospheric methane. *Proceedings of the National Academy of Sciences of the United States of America*, *116*(17), 8515–8524. https://doi.org/10.1073/pnas.1817812116

Urquhart, S. G., Hitchcock, A. P., Priester, R. D., & Rightor, E. G. (1995). Analysis of polyurethanes using core excitation spectroscopy. Part II: Inner shell spectra of ether, urea and carbamate model compounds. *Journal of Polymer Science Part B: Polymer Physics*, *33*(11), 1603–1620. https://doi.org/10.1002/polb.1995.090331105

Vandehey, N. T., Northen, T. R., Brodie, E. L., & O'Neil, J. P. (2014). Noninvasive mapping of photosynthetic heterogeneity in biological soil crusts by positron emission tomography: Carbon fixation. *Environmental Science & Technology Letters*, *1*(10), 393–398. https://doi.org/10.1021/ez500209c

Walker, D. A., Epstein, H. E., Gould, W. A., Kelley, A. M., Kade, A. N., Knudson, J. A., Krantz, W. B., Michaelson, G., Peterson, R. A., Ping, C.-L., Raynolds, M. K., Romanovsky, V. E., & Shur, Y. (2004). Frost-boil ecosystems: Complex interactions between landforms, soils, vegetation and climate. *Permafrost and Periglacial Processes*, *15*(2), 171–188. https://doi.org/10.1002/ppp.487

Whalen, S. C., & Reeburgh, W. S. (1990). Consumption of atmospheric methane by tundra soils. *Nature*, *346*(6280), 160–162. https://doi.org/10.1038/346160a0

Wojdyr, M. (2010). *Fityk*: A general-purpose peak fitting program. *Journal of Applied Crystallography*, *43*(5), 1126–1128. https://doi.org/10.1107/S0021889810030499

Wolf, D. C., & Skipper, H. D. (2018). Soil sterilization. In R. W. Weaver, S. Angle, P. Bottomley, D. Bezdicek, S. Smith, A. Tabatabai, & A. Wollum (Eds.), *SSSA book series* (pp. 41–51). Soil Science Society of America. https://doi.org/10.2136/sssabookser5.2.c3

Yang, Z., Wullschleger, S. D., Liang, L., Graham, D. E., & Gu, B. (2016). Effects of warming on the degradation and production of low-molecular-weight labile organic carbon in an Arctic tundra soil. *Soil Biology and Biochemistry*, *95*, 202–211. https://doi.org/10.1016/j.soilbio.2015.12.022

Yu, G. (2020). Using ggtree to visualize data on tree-like structures. *Current Protocols in Bioinformatics*, *69*(1). https://doi.org/10.1002/cpbi.96

Zhang, Q., Yang, G., Song, Y., Kou, D., Wang, G., Zhang, D., Qin, S., Mao, C., Feng, X., & Yang, Y. (2019). Magnitude and drivers of potential methane oxidation and production across the Tibetan alpine permafrost region. *Environmental Science & Technology*, *53*(24), 14243–14252. https://doi.org/10.1021/acs.est.9b03490

SUPPORTING INFORMATION

Additional supporting information may be found in the online version of the article at the publisher's website.

How to cite this article: Schmidt, M. P., Mamet, S. D., Senger, C., Schebel, A., Ota, M., Tian, T. W., Aziz, U., Stein, L. Y., Regier, T., Stanley, K., Peak, D., & Siciliano, S. D. (2022). Positron-emitting radiotracers spatially resolve unexpected biogeochemical relationships linked with methane oxidation in Arctic soils. *Global Change Biology*, *00*, 1–14. https://doi.org/10.1111/gcb.16188